

Interfacial geometry dependence of the iron magnetic moment: The case of MgO/Fe/MgOJuan Ignacio Beltrán,^{1,*} Lluís Balcells,² and Carlos Martínez-Boubeta³¹*Departamento de Física Teórica de la Materia Condensada, Universidad Autónoma de Madrid, Madrid 28049, Spain*²*Instituto de Ciencia de Materiales de Barcelona (ICMAB-CSIC), Campus UAB, Bellaterra 08193, Spain*³*Departament d'Electrònica and IN2UB, Universitat de Barcelona, Barcelona 08028, Spain*

(Received 23 September 2011; revised manuscript received 9 December 2011; published 27 February 2012)

The prediction and experimental demonstration of a very large magnetoresistance in Fe/MgO/Fe tunnel junctions have led to intense study of related systems in the last decade. In the present paper, we concentrate on the role of interface coordination, Fe thickness, and magnetization in the MgO/Fe/MgO mirror. By first-principles analysis, it is shown that the iron magnetic moment can rise up to $4 \mu_B$, accounting for observed deviation of the Fe atoms in the vicinity of MgO interfaces. The origin is attributed to site preference predicted by our calculations, namely, that, unlike the case of Fe atoms in the monolayer range sitting just above the oxygen atoms of the MgO(001) substrate, the charge transfer induced by the O *p-d* Fe interaction leads to a structural distortion that stabilizes the Mg at the very first deposition stages of the capping layer, facing Fe sites.

DOI: 10.1103/PhysRevB.85.064417

PACS number(s): 75.70.-i, 75.40.Mg, 75.50.Bb

I. INTRODUCTION

The ability to control both the atomic structure and composition of hetero-interfaces is emerging as one of the major challenges for the development of novel electronic devices with a range of functional properties. In this regard, previous studies reported^{1,2} that the preferential tunneling of Δ_1 symmetry states in Fe/MgO/Fe(001) junctions would lead to magnetoresistance values in excess of 1000%. Such a huge value has not yet been obtained, but the tunneling magnetoresistance has gradually been increasing since then.³⁻⁵ Progress made in the last decade is the result of the study not only of the transport properties but a continuous effort in characterizing the MgO crystalline barrier, the chemical composition of the interface, and its electronic structure, which provide information on the spin polarization of the system.⁶⁻¹⁰ Yet, the nature of Fe at the MgO interface, with differences between the Fe/MgO and MgO/Fe cases in real systems,¹¹ is still under debate. For instance, one of the major consequences of the deposition of MgO on a metal surface is a shift in the metal work function.¹²⁻¹⁴ This metal-supported MgO barrier (such is the case for Fe/MgO) shows modified wetting properties, which can influence the structure and magnetization of the posterior Fe atoms deposited on top (thus modifying the Fe/MgO/Fe nominal symmetry).^{15,16} Accordingly, as theoretically predicted,¹⁷ the surface magnetism would be enhanced by about 30% compared with the bulk magnetic moment (mm) of $2.2 \mu_B$. From an experimental point of view, Koyano *et al.*¹⁸ confirmed the enhanced mm of the lattice-distorted Fe in polycrystalline Fe/MgO multilayered films. More recently, Sicot *et al.*¹⁹ studied the electronic and magnetic properties of Fe epitaxial monolayers (ML) in contact with a single-crystalline MgO(001) tunneling barrier using x-ray absorption spectroscopy and x-ray magnetic circular dichroism (XMCD) measurements. They tried to definitely demonstrate the enhancement of the Fe mm in contact with MgO by performing measurements on samples with the following architecture (from the substrate side): V(001) buffer/10 ML Co-bcc/1 ML Fe/MgO. Similar experiments were performed by Mamiya *et al.*²⁰ Values reach $3.0 \pm 0.3 \mu_B$ per Fe atom at room temperature (RT). So far, however, it has been difficult to separate

the different contributions of Co and MgO in the enhancement of the mm. These observations also provided evidence that the 1 ML Fe supported onto a metal (Co) is not oxidized at all, despite the Fe layer directly facing the MgO barrier. However, this argument may not apply for the case of Fe deposited onto MgO, given the importance to consider the actual charge transfer between Fe atoms and their surroundings,¹⁴ as discussed above. Indeed, electronic mixing^{17,21} and evidences for a FeO interface have been demonstrated but credited to be due to thermodynamic constraints.^{22,23}

Little attention has been given to the properties of the MgO/Fe/MgO system. In this paper, the effect of interfacial coordination on the structural and magnetic properties of Fe sandwiches is investigated via first-principles calculations. In agreement with experiments, a magnetic moment much higher than the bulk is demonstrated, which we expect to play an important role in the study of double tunnel junctions and samples exhibiting quantum confinement effects.^{24,25}

II. EXPERIMENT AND MODEL

We first measured the mm of ultrathin Fe films sandwiched between MgO layers in fully epitaxial (001) oriented structures consisting of a MgO(001) substrate/MgO (10 nm buffer)/Fe/MgO (10 nm capping). Details have been previously described.²⁶ Briefly, experiments were conducted on sputtered films deposited at RT in order to avoid three-dimensional island growth and minimize interdiffusion. The thickness of the Fe layer was accurately determined by measuring the x-ray reflectivity. This technique has been proven to be especially sensitive in the case of symmetric structures, where the deposition of alternating layers of high (Fe) and low refractive index (MgO) creates interference fringes and drastic changes in the reflectivity, thus allowing for single-atomic-layer resolution. Magnetization was measured using available commercial superconducting quantum interference devices (SQUID) at RT and with a maximum magnetic field of 55 kOe applied parallel to the film plane. In all cases, the linear diamagnetic background from the MgO substrate and capping layers has been properly subtracted.²⁷ In Fig. 1, we present the plot

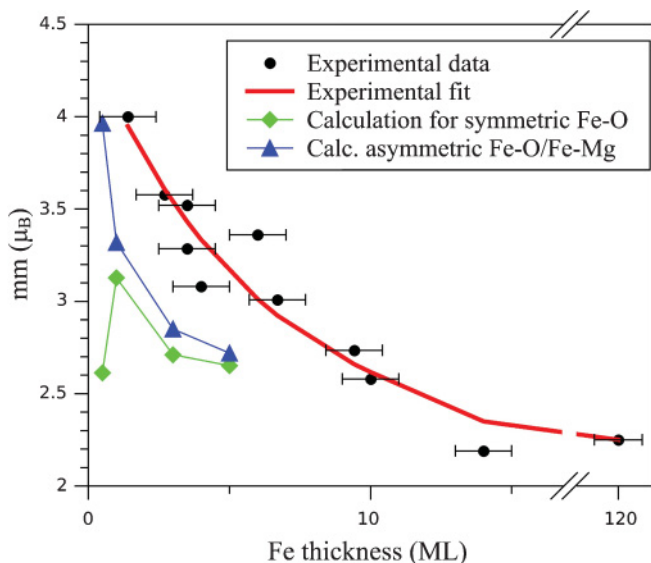


FIG. 1. (Color online) Magnetic moment averaged per Fe atom from SQUID measurements (black circles), together with theoretical calculations of MgO/Fe/MgO structures with symmetric Fe-O bonding (green diamonds), and asymmetric coordination (blue triangles), as a function of the Fe thickness. The experimental data are fitted to a phenomenological exponential decaying function (as $mm = mm_{\text{bulk}} + mm_{\text{surface}} e^{1-\text{thickness}/k}$, with the characteristic decay length $k = 6$ ML), which converge at large coverage to bulk Fe values.

of the experimental mm at saturation, averaged per Fe atom, as a function of the Fe layer width, together with simulations of two different MgO(substrate)/Fe/MgO(capping) geometrical arrangements (see following). We find that mm is larger than the bulk value for the thinner films and monotonically decays with film thickness. Thus, it seems clear that a genuine surface mm enhancement is seen. It reaches about $4 \mu_B$, thus either indicating the valence state of iron to be closer to Fe^{2+} , as for the case of diluted iron impurities in MgO,²⁸ or the Fe atom to be bounded to Mg ions.²⁹ We should note that XMCD experiments in our samples³⁰ showed neither mm induced on the MgO due to the proximity of the ferromagnet, nor a multiplet structure indicative of iron oxidation. We surmise the answer to this dilemma depends on a complex interplay between the structural changes and the charge-transfer process at the interface.

We next used the semilocal density functional theory to investigate the magnetic properties of Fe layers facing MgO. Calculations were performed at the generalized-gradient approximation level, using the exchange-correlation functional developed by Perdew, Burke, and Ernzerhof.³¹ We employed the SIESTA code with its localized atomic orbital basis sets.³² Global structure optimization included a $6 \times 6 \times 6$ k -point mesh and an energy cutoff value of 300 Ry. The atoms within the supercell are relaxed by using a conjugate gradient minimization until the atomic forces are less than $0.1 \text{ eV}/\text{\AA}$. The settings of the calculation are described elsewhere.³³ Special attention was given to the thickness of the slab representing the MgO substrate and Fe layers, which have been shown to profoundly affect the calculated magnetic properties.³⁴ We have

TABLE I. Magnetic moment (mm) projected to the interfacial Fe and O ions in various slab structures. The stability of each system is expressed with respect to the total energy of the isolated constituents.

	Layers (ML)		mm (μ_B)		Distance (\AA) Fe-O	Stability (eV)
	MgO	Fe	Fe	O		
Superlattice	4	0.5	3.41	0.14	1.96	4.70
		1	3.23	0.09	2.05	3.26
	5	0.5	3.10	0.03	2.14	2.83
		1	3.31	0.05	2.30	1.41
		2	2.76	0.04	2.09	1.37
	6	3	2.71	0.04	2.07	-1.38
		5	2.68	0.07	2.02	-1.65
		1	3.51	0.15	1.95	3.48
	7	1	3.33	0.07	2.13	3.28
		0.5	2.98	0.01	2.11	2.50
		1	3.30	0.05	2.31	1.32
Thin film	4	0.5	3.94	0.11	2.06	4.15
		1	3.46	0.06	2.15	3.45
	5	0.5	4.01	0.10	2.06	3.88
		1	3.42	0.06	2.14	3.47
		2	2.75	0.04	2.06	2.36
	6	3	2.88	0.06	2.05	3.00
		5	2.84	0.05	2.05	3.19
		0.5	4.01	0.10	2.06	3.89
	1	3.40	0.06	2.13	3.42	

considered Fe coverages down to 0.5 ML, since in real samples, the interface cannot be perfectly flat (the MgO substrate steps being intrinsically higher than an Fe ML).²⁶ Two different slab structures were designed: a periodic thin film configuration separated by 15 \AA of vacuum, and superlattice arrangements. By changing the barrier width, we aimed to quantify the relative importance of the coordination determining the mm: superlattice structures with an even number of MgO monolayers consist of stacked layers alternating between those that contain only Fe atoms placed atop O atoms (Fe-O), consistent with the experimental data,^{35,36} and those in which the Fe is forced to bind to Mg (Fe-Mg). In contrast, for an odd number of MgO layers, the O interfacial ions always face the Fe atoms while Mg falls in hollow positions. Results showed substantial energy differences between different types of structures. For the superlattice, the different coordination affects each of the properties in Table I. Namely, stability is larger for an odd number of MgO layers, which implies that the Fe is preferentially located on the oxygen on-top site. However, in the thin film structure, there is no qualitative difference among the MgO coverage ranges. This is a result of the interface always being Fe-O coordinated and the interaction between the periodically repeated slabs being decoupled by the introduction of vacuum. Notably, we found good agreement of our mm values with earlier calculations for supported Fe layers or clusters onto MgO.^{16,17,37,38} For thicker Fe films, compensation of interface charge by the shallow Fe layers gradually decreases the enhancement of the surface magnetization towards the bulk Fe value.

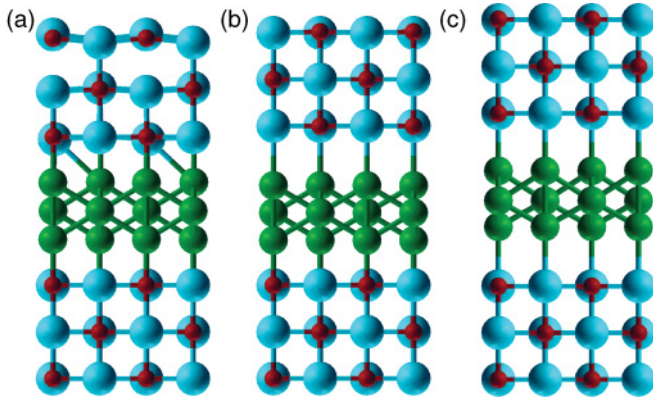


FIG. 2. (Color online) Schematics, from bottom to top, of the calculated crystalline structure for the MgO(substrate)/Fe/MgO(capping) case with 3 ML Fe facing oxygen ions at both interfaces (a), Fe binds to the O ions onto the substrate but to Mg in the capping layer (b), and Fe facing Mg at both sides (c). Small (red), big (blue), and medium (green) circles correspond to O, Mg, and Fe, respectively.

The interatomic distances along the out-of-plane (001) direction are also summarized in Table I. The interfacial Fe-O distances are found to be shorter than the distance in bulk FeO (2.154 Å).³⁹ Small mm oscillations in varying Fe and MgO thickness are also clearly illustrated. Curiously, spin-dependent electron reflectivity and the work function of the MgO thin films grown on Fe(001) have also been demonstrated to oscillate with MgO thickness.⁴⁰ We have, therefore, investigated the effect of interfacial chemical structure using MgO/Fe/MgO sandwiches. Three structures were considered: Fe facing oxygen ions at both the MgO/Fe and Fe/MgO interfaces (called hereafter “symmetric Fe-O”), Fe binds to the O ions onto the substrate but to Mg in the capping layer (“asymmetric Fe-Mg”), and Fe facing Mg at both sides

(referred to as “symmetric Fe-Mg”). The (001) in-plane MgO substrate lattice was fixed at the bulk value (optimized lattice parameter 4.27 Å), and the Fe and capping layers were matched epitaxially, as shown in Fig. 2.

For some of the configurations in Fig. 2, we show in Fig. 1 the mm as a function of the Fe layer width. The mm is large for the thin film structures and decays monotonically, showing a maximum for the smallest coverage, except for the symmetric Fe-O case. This situation arises because the interfacial properties are mostly driven by the Fe-O charge transfer, Fe being the electron donor and O being the acceptor, which is not full due to the reduced Fe coverage. The (non-)decaying trend corresponds to the Fe coverage that decreases (increases) the Fe averaged amount of electrons transferred to the O. Therefore, the maximum in Fig. 1 can be regarded as a compromise between an increase of mm due to ionicity and a decrease by the bulk-like character of thicker Fe coverages.

III. DISCUSSION AND CONCLUSION

We considered structural relaxations to account for the electronic response to the epitaxial in-plane strain. However, we could not find remarkable differences in magnetic moments among the relaxed and unrelaxed structures, suggesting the surface relaxation, and thus change in interlayer distance, only slightly contributes to the enhancement of magnetic moment, as already reported in Ref. 41. Figure 2 gives evidence for the oscillating relaxation and rumpling obtained for Fe/MgO(capping) in this procedure.⁴² Such rumpling mostly takes place in the Fe-O coordination, rather than in the Fe-Mg, and it is related to the interfacial charge transfer. This can be seen in Table II since the amount of O charge is clearly larger at the interfaces with Fe-O coordination. In fact, the structural distortion in the oxide film creates a dipole moment which partially compensates that due to the interfacial charge transfer. Note that there is almost no difference in the mm values for

TABLE II. Mulliken charges projected to the atoms of the MgO(substrate)|Fe and Fe|MgO(capping) interfaces for different Fe coverages, with the MgO thickness fixed to 3 ML. We also include the average magnetic moment per iron (mm), and stability of the MgO/Fe/MgO heterostructure regarding the constituent crystals.

	Fe ML	MgO Fe		Fe MgO		mm (μ_B)	Stability (eV)
		O	Fe	Fe	O		
Symmetric Fe-O	0.5	6.79/6.69	7.36	7.36	6.71/6.79	2.61	6.68
	1	6.77	7.29	7.29	6.77	3.13	6.88
	3	6.81	7.66	7.66	6.82	2.71	10.15
	5	6.82	7.66	7.67	6.82	2.65	15.94
Asymmetric Fe-Mg	0.5	6.67/6.68	7.34	7.34	6.70/6.80	3.96	7.41
	1	6.80	7.46	7.46	6.66	3.32	9.06
	3	6.82	7.70	7.85	6.67	2.84	12.72
	5	6.82	7.63	7.79	6.67	2.72	18.99
	8	6.82	7.64	7.90	6.69	2.74	30.77
	10	6.82	7.64	7.88	6.68	2.74	37.94
Symmetric Fe-Mg	0.5	6.69	7.46	7.46	6.69	3.99	8.51
	1	6.67	7.66	7.66	6.67	3.40	10.60
	3	6.82	7.71	7.84	6.67	2.85	12.73
	5	6.67	7.80	7.79	6.67	2.78	22.22

thicker Fe coverages (5, 8, and 10 ML). This saturation value, different from the experimental Fe bulk value of $2.26 \mu_B$, is due to the interfacial constraints imposed onto the in-plane lattice parameter matching that of the MgO substrate. This leads to an Fe cell dimension of 3.02 \AA , instead of the 2.87 \AA lattice constant of a body-centered cubic iron. We assessed accuracy of the computational method by conducting a series of calculations on Fe bulk. The optimum lattice constant of Fe bulk was calculated to be 2.87 \AA , with a magnetic moment of $2.34 \mu_B$. Accordingly, calculations in unsupported Fe crystals with a cell dimension of 3.02 \AA indicated that mm increases up to $2.71 \mu_B$. Thus, these results give us some confidence in the validity of our model for the case of Fe ultrathin distorted films grown epitaxially onto substrates.

Regarding epitaxial stability, a summary of the total energy for each of the interface coordinations is shown in Table II. One can clearly see that the “symmetric Fe-O” coordination is more stable than any of the Fe-Mg ones. However, the stability difference between the “symmetric Fe-O” and “asymmetric Fe-Mg” increases by increasing the Fe coverage, being only about 0.7 eV for the 0.5 Fe ML case. Besides, we have calculated the total energy for intermediate 1 and 2 ML MgO cappings, which have stability values of 7.72 and 6.88 eV for the “symmetric Fe-O,” while values are 6.77 and 7.55 eV for the “asymmetric Fe-Mg.” Importantly, this indicates that the most stable location for the magnesium atoms is on top of Fe for the first MgO layer. The reasons underlying the Fe-Mg stability, however, still remain open. Whereas the parameter of interest is often the optimal interface separation for which the total energy is minimal, one needs to remember that at a realistic interface, significant numbers of atoms are located off their preferential adsorption site and/or at distances different from those estimated in model calculations, as already pointed out for the Mo(001)/MgO case.⁴³ *In-situ* scanning tunneling microscopy would be highly valuable to confirm this point. For instance, studies on two-dimensional Fe islands onto MgO(001) demonstrated that hardly any atom is occupying the energetically most favorable fourfold hollow sites of the bcc lattice,⁴⁴ where the majority of atoms are displaced to less favorable sites, which might facilitate Fe above Mg ions. In addition, *ab initio* studies also confirmed that the adsorption

energy of Fe at oxygen-defect sites, with four nearest Mg neighbors, is slightly lower than that of Fe on top of the surface O atom of stoichiometric MgO(001).⁴⁵ It is also worth mentioning that the metallic Mg insertion layer between the MgO barrier and a bottom magnetic layer is known to be efficient for increasing the magnetoresistance ratio and for reducing the device resistance area product.⁴⁶ We note that changes in the MgO barrier as a function of high-temperature annealing (an indispensable step to obtain giant tunneling magnetoresistance above 100% in MgO-based junctions) have been extensively studied. Annealing is found to decrease the resistance of the junction, although the effective barrier layer width expands.⁴⁷ This paradox is usually explained as being due to a reduction of the density of oxygen vacancies, though the resulting similarities with the Mg insertion layer case might point to their common origin. Please note that Mg can diffuse easily at the temperatures involved here, producing a Mg enrichment at the MgO surface.⁴⁸ We surmise that by applying the correct deposition kinetics, or postgrowth annealing, the thermodynamics can favor certain percentage of Fe-Mg coordinated interface, as it is considered here in order to properly explain the exponential decrease of the averaged Fe mm while increasing the Fe coverage, as depicted in Fig. 1. We stress that the phenomenon described here probably has an influence only on the first stages of the nucleation process.

The drop of the magnetic moment for the symmetric Fe-O case is also worth noting here (Fig. 1). The same sensitive dependence of the mm of the interfacial layer is reported for Fe/V/MgO and Fe/Co heterostructures.^{49,50} In the following, we provide a qualitative understanding of this finding. On the one hand, our calculations suggest hybridization of Fe $3d$ with O $2p$ states, where the electronic structure of both Fe and O resemble the state of FeO, which explains the formation of polarized oxygen-derived states usually found at the Fe-MgO interface.^{21,40,51} In this regard, Fe was previously calculated to induce a mm of $0.2 \mu_B$ on the oxygen sites at the interface,^{52,53} while experimental results from Bowen *et al.*³⁰ suggested induced moments no greater than $0.05 \mu_B$. This trend is reproduced by our *ab initio* calculations, as can also be seen in Table I.

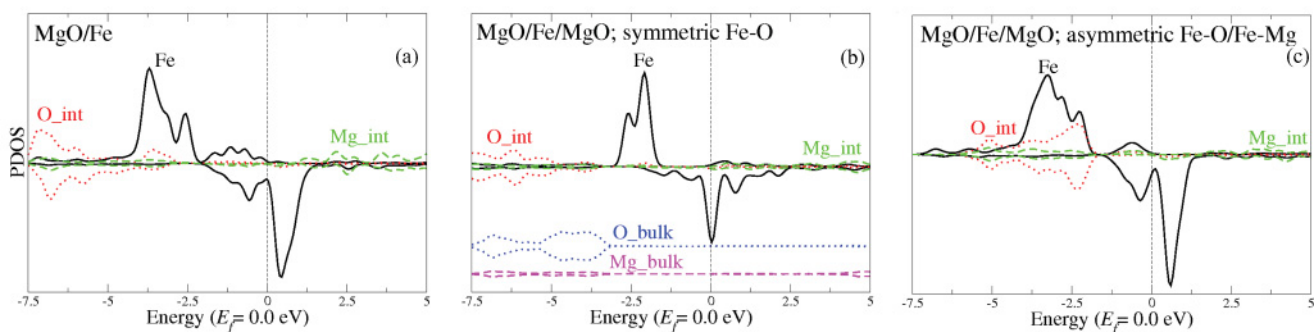


FIG. 3. (Color online) Projected DOS over the atoms at the interface (Fe, Mg_{int}, and O_{int}) and at inner layers (Mg_{bulk}, O_{bulk}) for different structures consisting of 0.5 ML Fe and 3 ML MgO , where upwards (downwards) curves correspond to majority (minority) spins. The Fermi level (E_f), depicted with dashed vertical lines, is set to zero for all plots. Solid, dotted, and dashed lines correspond to Fe, O, and Mg atoms, respectively. (a) Corresponds to the MgO/Fe structure with Fe-O coordination, (b) to the conventional MgO/Fe/MgO structure with Fe atoms facing O ions, while in (c) the capping layer sits its Mg ions upon the iron.

TABLE III. Magnetic moment (mm) for the interfacial atoms in MgO(3 ML)/Fe/FeO(1 ML)/MgO(3 ML), stabilities for each structure, and averaged mm. 5** corresponds to the case allowing for full relaxation of the atoms.

	Fe ML	MgO Fe		Fe FeO		FeO MgO		mm (μ_B)	Stability (eV)
		O	Fe	Fe	Fe(FeO)	O(FeO)	O(MgO)		
Symmetric Fe-O	0.5	0	2.69	2.69	3.59/3.56	0.11/0.21	0.02/0.03	2.69	5.89
	1	0	2.74/2.88	2.74/2.88	3.46/3.43	0.13/0.17	0.02/0.03	2.81	6.19
	3	0.03	3.08	2.98/2.99	3.47/3.44	0.19/0.19	0.03/0.04	2.96	11.77
	5	0.03	3.07	2.91	3.43/3.46	0.19	0.05/0.04	2.86	19.38
	5**	0.03	2.86	2.69	3.40	0.20	0.05/0.04	2.69	16.21
Asymmetric Fe-O/Fe-Mg	0.5	0.05	2.69	2.69	3.54/3.52	0.18/0.27	0.00	2.69	6.79
	1	0.02	2.61/2.59	2.61/2.59	3.38/3.43	0.18	0.01	2.60	7.12
	3	0.04	2.812	2.71	3.42/3.43	0.21	0.01	2.75	12.42
	5	0.03	3.06	2.91	3.43/3.45	0.19	0.04	2.86	19.39

We depict in Fig. 3 the projected density of states (PDOS) for the MgO/Fe thin film and MgO/Fe/MgO structures showing Fe-O and Fe-Mg interfacial coordination. The PDOS for the “bulk-like” atoms (Mg_bulk, and O_bulk) is only included for the MgO/Fe/MgO structure with Fe-O coordination, since we found it is similar among the three calculations, meaning the models employed provide a common bulk electronic structure as reference. Regarding the Fe contribution, we can see that Figs. 3(a) and 3(c) share qualitatively similar features, as a result of the charge smoothly extending into the vacuum region for the thin film case.¹⁷ On the other hand, the situation is very different in Fig. 3(b), where the Fermi level is located at the minority peak, and therefore the spin polarization (and mm) is much lesser than in the former cases. We recognize a striking similarity in our results with those published by Shimabukuro *et al.*⁵⁴ In this regard, the interfacial perpendicular anisotropy in 3d transition metals adjacent to a MgO barrier has attracted considerable attention for its relevance to voltage-driven spintronics applications with low power consumption.⁵⁵ Although not properly understood at this time, the close correlation between this perpendicular anisotropy and the drop in magnetization for overoxidized structures probably indicates that both have the very same origin, i.e., *p-d* hybridization near Fermi level. Obviously, further work is required before firm conclusions can be drawn.

The previous results hold for perfectly epitaxial interfaces. However, the structure of interfaces in real samples appears to be significantly different from the ideal model used in our calculations. On the one hand, when growing MgO by evaporation or sputtering deposition, a gas containing a majority of atomic species is generated.²² Since Mg is very volatile and O rapidly sticks to the metal surface,⁵⁶ FeO is likely to result when depositing MgO onto Fe. In this regard, spin-polarized experiments⁵⁷ have previously highlighted the important role of stoichiometry in MgO/Fe(001). Therefore, in order to complete the study and the comparison between experiments and theory, let us focus on the MgO(001)/Fe/FeO/MgO structure where a 1 FeO ML is intercalated between the Fe slab and the MgO capping layer. The results are shown in Table III. It is noteworthy that, unlike in the MgO/Fe/MgO structure, when inserting an FeO layer, the most stable coordination is Fe facing O at both interfaces, which also provides the larger mm. It is also observed that the mm induced in the oxygen

ions is negligible, except for those of the FeO layer, which often show two values due to the corrugation that arises from the interfacial charge displacements. It is interesting to see that the Fe mm increases by increasing the Fe thickness for both the MgO(substrate)/Fe and Fe/FeO interfaces, reaching a value close to 3 μ_B . Here, the role of the FeO layer is to support a rather constant and high value of mm through the entire Fe slab at least up to 5 ML. These findings indicate that the MgO/Fe/FeO/MgO structure is a good candidate for the realization of double tunnel junctions,^{58,59} since the most stable interface configuration holds a relatively high mm value due to the incorporation of FeO. To assess the validity of our results, we have also considered the relaxed structure of the supercell, meaning that the substrate lattice parameter is not fixed to the MgO constant. We observed that relaxation reduces the mm compared to the “constrained” 5 ML. This stems from the charge transfer at the interface, showing a charge reduction on Fe (electron donor) and a slight enhancement on the O (acceptor). This result is similar to that for the MgO/Fe/MgO structure with Fe-O coordination, where relaxation at the interface results in smaller mm.

In summary, we have performed a systematic study aiming at the understanding of the mm values of MgO/Fe/MgO structures. Results show that at the very first deposition stages for the capping layer, the most stable coordination is Fe facing Mg, instead of the Fe-O, being the two classes of interfaces substantially different from each other. Mainly, the Fe-Mg coordination helps diminish the detrimental effect of the Fe-O bonding, where a small amount of covalency originates from the 3d (Fe) 2p (O) hybridization (Fig. 3). Concomitant to this, the surface magnetization in Fe films is enhanced (Fig. 1). These results imply an interface model for magnetic tunnel junctions with asymmetric Fe-O/MgO/Mg-Fe layer stacking that is different from the ideal symmetric heterostructure, opening the path to a more accurate description and engineering of spintronic devices based on MgO barriers.

ACKNOWLEDGMENTS

C.M.B. is supported by the “Ramón y Cajal” program of Spain. The authors thank A. Cebollada, F. Illas, L. Giordano, and G. Pacchioni for stimulating discussions.

*juan.beltran@uam.es

- ¹W. H. Butler, X.-G. Zhang, T. C. Schulthess, and J. M. MacLaren, *Phys. Rev. B* **63**, 054416 (2001).
- ²J. Mathon and A. Umerski, *Phys. Rev. B* **63**, 220403(R) (2001).
- ³M. Bowen, V. Cross, F. Petroff, A. Fert, C. Martínez-Boubeta, J. L. Costa-Krämer, J. V. Anguita, A. Cebollada, F. Briones, J. M. de Teresa, L. Morellón, R. Ibarra, F. Güell, F. Peirò, and A. Cornet, *Appl. Phys. Lett.* **79**, 1655 (2001).
- ⁴S. Yuasa, T. Nagahama, A. Fukushima, Y. Suzuki, and K. Ando, *Nat. Mater.* **3**, 868 (2004).
- ⁵S. Ikeda, J. Hayakawa, Y. Ashizawa, Y. M. Lee, K. Miura, H. Hasegawa, M. Tsunoda, F. Matsukura, and H. Ohno, *Appl. Phys. Lett.* **93**, 082508 (2008).
- ⁶M. Müller, F. Matthes, and C. M. Schneider, *J. Appl. Phys.* **101**, 09G519 (2007).
- ⁷L. Plucinski, Y. Zhao, B. Sinkovic, and E. Vescovo, *Phys. Rev. B* **75**, 214411 (2007).
- ⁸G. X. Miao, Y. J. Park, J. S. Moodera, M. Seibt, G. Eilers, and M. Münzenberg, *Phys. Rev. Lett.* **100**, 246803 (2008).
- ⁹Y. Ke, K. Xia, and H. Guo, *Phys. Rev. Lett.* **105**, 236801 (2010).
- ¹⁰J. M. Teixeira, J. Ventura, J. P. Araujo, J. B. Sousa, P. Wisniowski, S. Cardoso, and P. P. Freitas, *Phys. Rev. Lett.* **106**, 196601 (2011).
- ¹¹F. J. Palomares, C. Munuera, C. Martínez Boubeta, and A. Cebollada, *J. Appl. Phys.* **97**, 036104 (2005)
- ¹²J. Goniakowski and C. Noguera, *Interface Sci.* **12**, 93 (2004).
- ¹³T. Jaouen, G. Jézéquel, G. Delhaye, B. Lépine, P. Turban, and P. Schieffer, *Appl. Phys. Lett.* **97**, 232104 (2010).
- ¹⁴T. Susaki, A. Makishima, and H. Hosono, *Phys. Rev. B* **83**, 115435 (2011).
- ¹⁵D. Ricci, A. Bongiorno, G. Pacchioni, and U. Landman, *Phys. Rev. Lett.* **97**, 036106 (2006).
- ¹⁶U. Martinez, G. Pacchioni, and F. Illas, *J. Chem. Phys.* **130**, 184711 (2009).
- ¹⁷C. Li and A. J. Freeman, *Phys. Rev. B* **43**, 780 (1991).
- ¹⁸T. Koyano, Y. Kuroiwa, E. Sita, N. Saegusa, K. Ohshima, and A. Tasaki, *J. Appl. Phys.* **64**, 5763 (1988).
- ¹⁹M. Sicot, S. Andrieu, F. Bertran, and F. Fortuna, *Phys. Rev. B* **72**, 144414 (2005).
- ²⁰K. Mamiya, T. Koide, Y. Ishida, Y. Osafune, A. Fujimori, Y. Suzuki, T. Katayama, and S. Yuasa, *Rad. Phys. Chem.* **75**, 1872 (2006).
- ²¹C. Martínez-Boubeta, Ll. Balcells, C. Monty, P. Ordejon, and B. Martínez, *Appl. Phys. Lett.* **94**, 062507 (2009).
- ²²J. L. Vassent, A. Marty, B. Gilles, and C. Chatillon, *J. Cryst. Growth* **219**, 444 (2000).
- ²³H. Oh, S. B. Lee, J. Seo, H. G. Min, and J.-S. Kim, *Appl. Phys. Lett.* **82**, 361 (2003).
- ²⁴A. Iovan, S. Andersson, Yu. G. Naidyuk, A. Vedyayev, B. Dieny, and V. Korenivski, *Nano Lett.* **8**, 805 (2008).
- ²⁵C. Martínez-Boubeta, Ll. Balcells, and A. Cebollada, *Appl. Phys. Lett.* **88**, 132511 (2006).
- ²⁶C. Martínez-Boubeta, C. Clavero, J. M. García-Martín, G. Armelles, A. Cebollada, Ll. Balcells, J. L. Menéndez, F. Peiró, A. Cornet, and M. F. Toney, *Phys. Rev. B* **71**, 014407 (2005).
- ²⁷J. Orna, P. A. Algarabel, L. Morellón, J. A. Pardo, J. M. de Teresa, R. López Antón, F. Bartolomé, L. M. García, J. Bartolomé, J. C. Cezar, and A. Wildes, *Phys. Rev. B* **81**, 144420 (2010).
- ²⁸T. Haupricht, R. Sutarto, M. W. Haverkort, H. Ott, A. Tanaka, H. H. Hsieh, H.-J. Lin, C. T. Chen, Z. Hu, and L. H. Tjeng, *Phys. Rev. B* **82**, 035120 (2010).
- ²⁹V. M. Medel, J. U. Reveles, S. N. Khanna, V. Chauhan, P. Sen, and A. W. Castleman, *PNAS* **108**, 10062 (2011).
- ³⁰M. Bowen, V. Cros, H. Jaffrès, P. Bencok, F. Petroff, and N. B. Brookes, *Phys. Rev. B* **73**, 012405 (2006).
- ³¹J. P. Perdew, K. Burke, and M. Ernzerhof, *Phys. Rev. Lett.* **77**, 3865 (1996).
- ³²J. M. Soler, E. Artacho, J. D. Gale, A. García, J. Junquera, P. Ordejón, and D. Sánchez-Portal, *J. Phys.: Condens. Matter* **14**, 2745 (2002).
- ³³J. I. Beltrán and M. C. Muñoz, *Phys. Rev. B* **78**, 245417 (2008).
- ³⁴O. Šipr, S. Bornemann, J. Minár, and H. Ebert, *Phys. Rev. B* **82**, 174414 (2010).
- ³⁵T. Kanaji, T. Kagotani, and S. Nagata, *Thin Solid Films* **32**, 217 (1976).
- ³⁶H. L. Meyerheim, R. Popescu, J. Kirschner, N. Jedrecy, M. Sauvage-Simkin, B. Heinrich, and R. Pinchaux, *Phys. Rev. Lett.* **87**, 076102 (2001).
- ³⁷M. C. Desjonquères, C. Barreteau, G. Autès, and D. Spanjaard, *Phys. Rev. B* **76**, 024412 (2007).
- ³⁸G.-X. Ge, Q. Jing, Z.-Q. Yang, and Y.-H. Luo, *Chin. Phys. Lett.* **26**, 083101 (2009).
- ³⁹K. Nakamura, T. Akiyama, T. Ito, M. Weinert, and A. J. Freeman, *Phys. Rev. B* **81**, 220409(R) (2010).
- ⁴⁰Y. Z. Wu, A. K. Schmid, and Z. Q. Qiu, *Phys. Rev. Lett.* **97**, 217205 (2006).
- ⁴¹T. Shimada, Y. Ishii, and T. Kitamura, *Phys. Rev. B* **81**, 134420 (2010).
- ⁴²J. Goniakowski and C. Noguera, *Surf. Sci.* **323**, 129 (1995).
- ⁴³H. M. Benia, P. Myrach, N. Nilius, and H.-J. Freund, *Surf. Sci.* **604**, 435 (2010).
- ⁴⁴G. Wedler, C. M. Schneider, A. Trampert, and R. Koch, *Phys. Rev. Lett.* **93**, 236101 (2004).
- ⁴⁵B. D. Yu, *Phys. Rev. B* **71**, 193403 (2005).
- ⁴⁶K. Tsunekwa, D. D. Djayaprawira, M. Nagai, H. Maehara, S. Yamagata, N. Watanabe, S. Yuasa, Y. Suzuki, and K. Ando, *Appl. Phys. Lett.* **87**, 072503 (2005).
- ⁴⁷Y. Liu, A. N. Chiaramonti, D. K. Schreiber, H. Yang, S. S. P. Parkin, O. G. Heinonen, and A. K. Petford-Long, *Phys. Rev. B* **83**, 165413 (2011).
- ⁴⁸J. F. Anderson, M. Kuhn, U. Diebold, K. Shaw, P. Stoyanov, and D. Lind, *Phys. Rev. B* **56**, 9902 (1997).
- ⁴⁹X. Feng, O. Bengone, M. Alouani, I. Rungger, and S. Sanvito, *Phys. Rev. B* **79**, 214432 (2009).
- ⁵⁰B. Swinnen, J. Meererschaut, J. Dekoster, G. Langouche, S. Cottenier, S. Demuyne, and M. Rots, *Phys. Rev. Lett.* **78**, 362 (1997).
- ⁵¹A. Cattoni, D. Petti, S. Brivio, M. Cantoni, R. Bertacco, and F. Ciccacci, *Phys. Rev. B* **80**, 104437 (2009).
- ⁵²E. Yu. Tsymlal, I. I. Oleinik, and D. G. Pettifor, *J. Appl. Phys.* **87**, 5230 (2000).
- ⁵³X.-G. Zhang, W. H. Butler, and Amrit Bandyopadhyay, *Phys. Rev. B* **68**, 092402 (2003).

- ⁵⁴R. Shimabukuro, K. Nakamura, T. Akiyama, and T. Ito, *Physica E* **42**, 1014 (2010).
- ⁵⁵Y. Shiota, T. Nozaki, F. Bonell, S. Murakami, T. Shinjo, and Y. Suzuki, *Nat. Mater.* **11**, 39 (2012).
- ⁵⁶G. Geneste, J. Morillo, F. Finocchi, and M. Hayou, *Surf. Sci.* **601**, 5616 (2007).
- ⁵⁷M. Müller, F. Matthes, and C. M. Schneider, *EPL* **80**, 17007 (2007).
- ⁵⁸T. Nozaki, A. Hirohata, N. Tezuka, S. Sugimoto, and K. Inomata, *Appl. Phys. Lett.* **86**, 082501 (2005).
- ⁵⁹D. Herranz, F. G. Aliev, C. Tiusan, M. Hehn, V. K. Dugaev, and J. Barnas, *Phys. Rev. Lett.* **105**, 047207 (2010).